Quantum-inspired particle swarm optimization algorithm with performance evaluation of fused images

Zhang Le[1], Zhang Xinman[1], Xu Xuebin[1*], Wang Dong[2], Liu Jie[2], Liu Yang[2]

[1]MOE Key Lab for Intelligent Networks and Network Security,
 School of Electronics and Information Engineering, Xi'an Jiaotong University,
 Xi'an, 710049, China

[2]Huawei Central Research Academy,
 Beijing, 100095, China

*Corresponding author: ccp9999@126.com

In order to improve and accelerate the speed of image integration, an optimal and intelligent method for multi-focus image fusion is presented in this paper. Based on particle swarm optimization and quantum theory, quantum particle swarm optimization (QPSO) intelligent search strategy is introduced in salience analysis of a contrast visual masking system, combined with the segmentation technique. The superiority of QPSO is quantum parallelism. It has stronger search ability and quicker convergence speed. When compared with other classical or novel fusion methods, several metrics for image definition are exploited to evaluate the performance of all the adopted methods objectively. Experiments are performed on both artificial multi-focus images and digital camera multi-focus images. The results show that QPSO algorithm is more efficient than non-subsampled contourlet transform, genetic algorithm, binary particle swarm optimization, *etc*. The simulation results demonstrate that QPSO is a satisfying image fusion method with high accuracy and high speed.

Keywords: multi-focus image fusion, quantum particle swarm optimization, perfect reconstruction, superior speed.

1. Introduction

Usually, the cameras used in current computer vision systems have the problem of a limited depth of field. As a result, in an image captured from these sensors, objects within the depth of field are focused clearly, while other objects are blurred. The purpose of multi-focus image fusion is to synthesize an image with every object in focus. It is a convenient and effective technique to fuse different focused images taken from the same scene into a new clearer one. The new fused image is quite

useful for human or machine perception. In the past decades, it has been widely adopted in computer vision, remote sensing, medical image processing, and military purposes, *etc*. [1, 2].

A wide variety of techniques have been studied in multi-focus image fusion. The techniques developed in the early days are based on multi-resolution approaches, which usually employ discrete wavelet transform (DWT) and various pyramid algorithms such as Laplacian pyramid, contrast-pyramid and wavelet-pyramid, *etc*. The basic idea is to perform a multi-resolution decomposition on each source image, then integrate all these decompositions to form a composite representation, and finally reconstruct the fused image by performing an inverse multi-resolution transform [2]. Especially, DWT is a superior representative method.

In recent years, some other innovative methods are commonly used in multi-focus image fusion. For example, curvelet transform (CT) is suitable for analyzing image edges such as curve and line characteristics. Non-subsampled contourlet transform (NSCT) is a shift-invariant version of the CT [3]. Besides, a pulse coupled neural networks (PCNN) model becomes popular since it has the advantages of processing information similar to the mode of human visual processing, and the global coupling and pulse synchronization of neurons that benefit image fusion with local image information [4, 5]. However, all these above methods that belong to pixel-based will produce more or less errors in the fusion results, as a very small error in registration results in mismatch of all the pixels in consideration. Region-based techniques are better in this respect [6]. Several novel algorithms have been applied in multi-focus image fusion to optimize the block size by heuristic search, making fusion a better performance.

A genetic search strategy called GA (genetic algorithm) was introduced into multi-focus image fusion by Zhang *et al*. [6, 7]. Later, they introduced a new fusion method – binary particle swarm optimization (BPSO). Lots of image experiments reveal that the two methods perform well both in zero reconstruction and increasing the fusion quality of multi-focus images [6, 7]. Nevertheless, we expect efficient fusion on the basi of good reconstruction results as far as possible. Currently, a different intelligent particle swarm inspired by quantum mechanism (QPSO – quantum particle swarm optimization) is proposed. The algorithm is globe convergent and has fast executing time. In this paper, we adopt this new method in multi-focus image fusion. The results of numerous fusion experiences show that QPSO achieves super performance in both fusion effect and fusion speed. Especially for processing pictures of big size, it can save a lot of time obviously.

This paper is organized as follows: Section 2 describes QPSO fusion algorithm for completeness, and gives out a schematic diagram detailing the steps. Section 3 lists the measures we suggested, which specially describe the definition of multi-focus images. The parts in Section 4 carry out the experimental results and analysis on artificial multi-focus images and digital camera multi-focus images, respectively. Finally the paper is concluded in the last section.

2. Multi-focus image fusion scheme based on QPSO search

In this section, first we adopt a contrast visual masking principle applied in multi-focus image fusion, which states how all the clear regions are selected to synthesize a fusion image. QPSO is an intelligence optimization search technique to choose the best block decomposition and accelerate the block searching process in the iterations of fusion. Here the basic algorithm QPSO is introduced. Also, the detailed process and procedure of QPSO fusion algorithm are presented.

2.1. Contrast visual masking principle [7]

In human vision system, the definition of focus images is tested by a uniform parameter, which can balance the deviations between the block pixel and the block mean. Consider an image I as a two-dimensional array of pixels, and the pixel in the i-th row and the j-th column shall be denoted by $I(i, j)$. With this notation, we define d_k, the uniform parameter of the partition block of an image I as follow:

$$d_k = \frac{1}{m \times n} \sum_{(i,j) \in B_k} \frac{|I(i,j) - \mu_k|}{\mu_k} \tag{1}$$

where μ_k is the mean of the image block B_k, and $m \times n$ is the block size.

In multi-focus image fusion, input images A and B are divided into non-overlapping blocks sized of $m \times n$. The i-th blocks of A and B images are denoted by A_i and B_i, respectively. Then image fusion is performed based on the uniform parameter of each block. Construct the i-th block F_i of the fused image as:

$$F_i = \begin{cases} A_i & \mathrm{d}A_i > \mathrm{d}B_i \\ B_i & \text{otherwise} \end{cases} \tag{2}$$

where $\mathrm{d}A_i$ and $\mathrm{d}B_i$ are uniform parameters of the relative block A_i and B_i of two input images A and B, respectively. The contrast visual masking model is to select the clearer regions from source images to merge the image F.

2.2. QPSO search fusion algorithm

Quantum particle swarm optimization algorithm is inspired by the concept and principle of quantum computing, which has stronger search ability and quicker convergence speed than conventional evolutionary algorithms. In a quantum mechanism system, each single particle has quantum behavior. Different from PSO, a quantum bit is used as probabilistic representation of particles, defined as the smallest information unit. By the action of a quantum rotation gate, particles can be in any linear superposition state of 0 and 1, but not only in the normal state 0 or 1, which increases the population individual diversity [8, 9].

In the standard particle swarm algorithm, particles converge to a rail form. It is easy for particles to search at a fixed area with limited speed. While in quantum particle swarm algorithm (QPSO), the search range is the whole quantum space. Particles can search the whole feasible solution space with a certain probability. In evolution equations of QPSO, the velocity vector is omitted. So it is easy to control with fewer parameters [10].

The steps of QPSO method are presented as follows:

1. Initialize the population of a particle swarm and the position of each particle. Determine the proper population number W and initialize the position of each particle by a stochastic method. The individuals of the population consist of two parameters corresponding to length m and width n of the optimal block size for the desired fused image. Suppose for an image of size $M \times N$, the search range is $(1, M-1)$ and $(1, N-1)$ in simplicity, so the position of the i-th particle C_i is coded as follows, composed of block's length and width:

$$C_i = \begin{bmatrix} n_{i,\,u+v} & n_{i,\,u+v-1} & \cdots & n_{i,\,u+2} & n_{i,\,u+1} & m_{i,\,u} & m_{i,\,u-1} & \cdots & m_{i,\,2} & m_{i,\,1} \end{bmatrix} \quad (3)$$

where u refers to the position row code length (of size $\log_2 M$), v refers to the position column code length (of size $\log_2 N$), and i belongs to a range of $[1, W]$ [6].

2. Evaluate the population and calculate each particle's fitness value. First, the input images A and B are divided into non-overlapping blocks with the size of $m \times n$. After applying a contrast visual masking model for each corresponding block of the source images, calculate the fitness value of the fused image by employing the spatial frequency (SF). The larger SF is, the more advantageous the corresponding particle's position is, and the more possible to search its surrounding areas it is.

3. Use QPSO search strategy to find new solutions. In the quantum particle swarm optimization problem, in D-dimensional space with W particles, the i-th particle's position at the $(t+1)$-th iteration is updated by these following equations:

$$x_{ij}^{t+1} = p_{ij}^{t+1} + \beta \, \mathrm{abs}\left(\mathrm{mbest}_j^t - x_{ij}^t\right) \ln\left(\frac{1}{u_{ij}^t}\right) \qquad \text{if} \qquad u \geq 0.5 \qquad (4)$$

$$x_{ij}^{t+1} = p_{ij}^{t+1} - \beta \, \mathrm{abs}\left(\mathrm{mbest}_j^t - x_{ij}^t\right) \ln\left(\frac{1}{u_{ij}^t}\right) \qquad \text{if} \qquad u < 0.5 \qquad (5)$$

where mbest showed in Eq. (6) denotes the mean value of personal best positions of all particles; p_{ij}^t is the local attractor, which is calculated as Eq. (7). The parameter β is called the contraction-expansion coefficient, which can be tuned to control the convergence speed of algorithm. It is defined in Eq. (8). Parameter μ is a random number distributed uniformly on $[0, 1]$

$$\mathrm{mbest}^t = \left(\frac{1}{W} \sum_{i=1}^{W} P_{i1}^t, \ \frac{1}{W} \sum_{i=1}^{W} P_{i2}^t, \ \ldots, \ \frac{1}{W} \sum_{i=1}^{W} P_{iD}^t \right) \qquad (6)$$

$$p_{ij}^t = \varphi_{ij}^t P_{ij}^t + \left(1 - \varphi_{ij}^t\right) P_{gj}^t \qquad \varphi \in U(0, 1) \tag{7}$$

$$\beta = \frac{0.5(\text{maxiter} - \text{count})}{\text{maxiter} + 0.5} \tag{8}$$

where W is the number of individuals in a population; φ is a random number distributed uniformly on [0, 1]; P_{ij}^t and P_{gj}^t represent the personal best position and the global best position in the t iteration; maxiter is the biggest population iteration times, and count is the current iteration time. Figure 1 shows how mbest and p_i update in detail. Each bit of mbest is determined by the number of 0 and 1 in the corresponding bit of personal best. If the number of 0 is more, the corresponding bit of mbest is 0, or it denoted by 1.
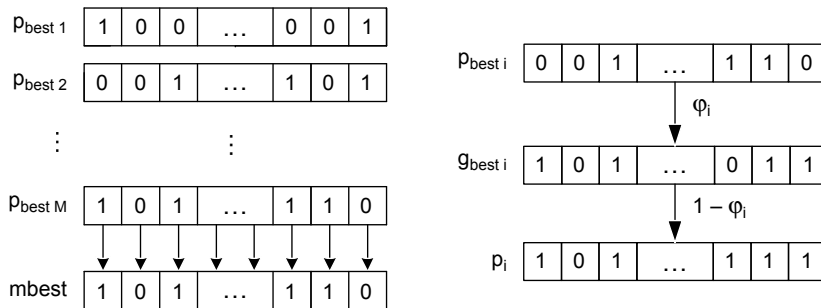

Fig. 1. Update of mbest and p_i.

4. Check whether the predefined stopping criterion is satisfied. If so, stop the algorithm and output the result, otherwise run to step 3. Here, the terminate condition is met when the operation reaches the maximum iteration, or the ratio of an average fitness value of present population to that of parent population locates in the interval [1, α]. The choice of α should ensure a good convergence speed of the algorithm and avoid the premature. In image vision applications, the optimal value of α is 1.005. The folding operation times are no more than $\log_2(MN/4)$ [6].
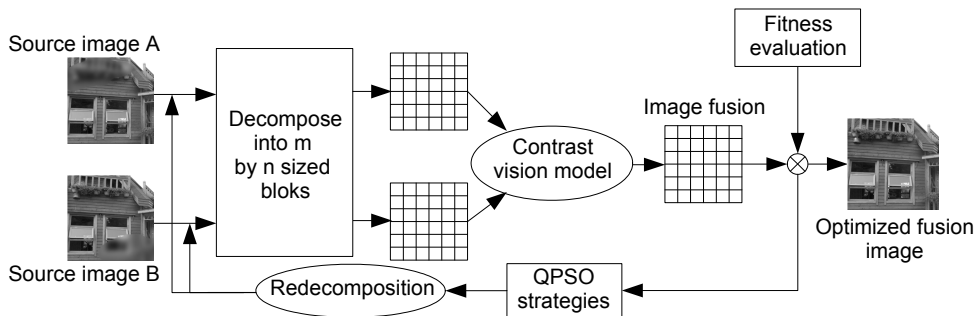

Fig. 2. Block diagram of the proposed multi-focus image fusion scheme.

5. Choose the optimized blocks to reach the best effect. Figure 2 illustrates the block diagram of the proposed multi-focus image fusion scheme.

The detailed procedure of QPSO search strategy is described as follows:

```
Initialize the population size, the positions, the dimensions of
the particles and the greatest folding operation times
For t = 1 → maximum iteration
   Compute the mean best position mbest of the population
   For i = 1 → population size W
   Compute the fitness function of each particle, respectively
   Update the individual best position P_i and the global best position P_g
   For j = 1 → dimension D
   Calculate the local attractor p_{ij}^t
   Update the position of particle
   End for
   End for
Judge whether the terminate condition is satisfied, if satisfied,
exit the loop
   End for
```

3. Evaluation criteria

To evaluate the overall performance of all the used algorithms on multi-focus image fusion, different assessment methods are studied in this paper to make the quantitative comparison that measure the quality of fusion image objectively. Metrics are used that can either employ or not employ a reference image. Moreover, time is employed as an important evaluation of the efficiency of fusion methods. Consider R is the reference image and F is the fused image. A and B are the two source images, respectively. They are all of size $M \times N$. $F(i, j)$ is the gray value of pixel at the position (i, j).

3.1. Root-mean-square error (RMSE) [11]

RMSE is the most valuable performance evaluation criterion when the reference image is available. It is defined as

$$\text{RMSE} = \sqrt{\frac{1}{M \times N} \sum_{i=1}^{M} \sum_{j=1}^{N} \left[R(i, j) - F(i, j) \right]^2} \tag{9}$$

If RMSE equals 0, it corresponds to perfect image reconstruction. Namely, the fused image is a perfect image, which has been achieved through accurate reconstruction of multi-focus images to the reference image.

3.2. Spatial frequency (SF) [12]

Spatial frequency indicates the overall active level of an image. At the same time it represents minus details of contrast and texture commutation characteristics. Spatial frequency could be used as a measure to quantify the clarity of image, which could

be calculated through the mean-square root of the spatial row frequency (RF) and the spatial column frequency (CF) as follows:

$$SF = \sqrt{RF^2 + CF^2} \tag{10}$$

where

$$RF = \sqrt{\frac{1}{M \times N} \sum_{i=1}^{M} \sum_{j=2}^{N} \left[F(i,j) - F(i, j-1) \right]^2} \tag{11}$$

$$CF = \sqrt{\frac{1}{M \times N} \sum_{j=1}^{N} \sum_{i=2}^{M} \left[F(i,j) - F(i-1, j) \right]^2} \tag{12}$$

Usually, a larger SF indicates that the image is clearer.

3.3. Energy of gradient (EOG) of the image [12]

Image gradient energy reflects the image gradient information. And, to some extent, it can be used to characterize the image characteristics and clarity gathered. The formula EOG is as follows:

$$EOG = \sum_{i=1}^{M} \sum_{j=1}^{N} \left[I_x^2(i,j) + I_y^2(i,j) \right] \tag{13}$$

Generally, the image is better with a larger value.

3.4. Mutual information (MI) [3]

Mutual information is a metric that measures the dependence degree of two images. It is defined as the sum of mutual information between each input image and the fused image

$$I_{AF} = \sum_{a,f} p_{AF}(i,j) \log \left[\frac{p_{AF}(i,j)}{p_A(i,j) p_F(i,j)} \right] \tag{14}$$

$$I_{BF} = \sum_{b,f} p_{BF}(i,j) \log \left[\frac{p_{BF}(i,j)}{p_B(i,j) p_F(i,j)} \right] \tag{15}$$

Thus the image fusion performance measure can be defined as

$$MI_F^{AB} = I_{AF} + I_{BF} \tag{16}$$

where p_{AF} is the jointly normalized histogram of A and F; p_A and p_B are the normalized histograms of A and F, respectively. The mutual information I_{BF} is similar to I_{AF}.

It indicates that MI measure reflects the total amount of information that the fused image F contains of A and B. Generally, the larger MI value is, the better the fusion result will be.

3.5. Transfer of edge information $Q^{AB/F}$ [3]

The $Q^{AB/F}$ is a metric which considers the amount of edge information transferred from the input images to the fused images. This method uses a sobel edge detector to calculate the strength and orientation information at each pixel in both source and fused images. $Q^{AB/F}$ is defined as follows:

$$Q^{AB/F} = \frac{\sum_{i=1}^{M} \sum_{j=1}^{N} \left[Q^{AF}(i,j) w^A(i,j) + Q^{BF}(i,j) w^B(i,j) \right]}{\sum_{i=1}^{M} \sum_{j=1}^{N} \left[w^A(i,j) + w^B(i,j) \right]} \quad (17)$$

where $Q^{AF}(i,j) = Q_x^{AF}(i,j) Q_y^{AF}(i,j)$; $Q_x^{AF}(i,j)$ and $Q_y^{AF}(i,j)$ are the edge strength and orientation preservation values, respectively. $Q^{BF}(i,j)$ is similar to $Q^{AF}(i,j)$. $w^A(i,j)$ and $w^B(i,j)$ are the influence parameters of $Q^{AF}(i,j)$ and $Q^{BF}(i,j)$, respectively. The dynamic range of $Q^{AB/F}$ is [0, 1]. A larger value implies better quality, and the ideal fusion should be $Q^{AB/F} = 1$.

4. Results and discussion

Experiments are performed on several sets of images to evaluate the proposed fusion algorithm and other typical methods. Both artificially produced and naturally acquired multi-focus images have been experienced by seven different fusion methods. All experiments have been done in a machine with Intel Core 4 processor 2.99 GHZ with 2 GB memory. The version of simulation software is Matlab 8.01.

4.1. Fusion of artificial multi-focus images

This experiment is conducted on a set of 8-bit gray level 256×256 sized images in Fig. 3 without overlapped blurred regions. It is assumed that they are fully registered before fusion. The house source images are focused either on the top or the bottom. A reference image is used to assess the quality of fusion image. It is hard to subjectively find the difference of fusion results among the seven algorithms. So we use RMSE to evaluate the overall performance of the different algorithms, and use SF, EOG to evaluate the definition of the fused images. In addition, MI and $Q^{AB/F}$ are employed to measure the transferred information obtained from source images. What is more, time is used as another important critical metric to test instantaneity of different methods.

Table 1 shows the fusion results of DWT, CT, NSCT and NSCT-PCNN methods. Considering the randomness of GA, BPSO and QPSO methods, 100 repeated runs are performed, and the average results are summarized in Tab. 2.
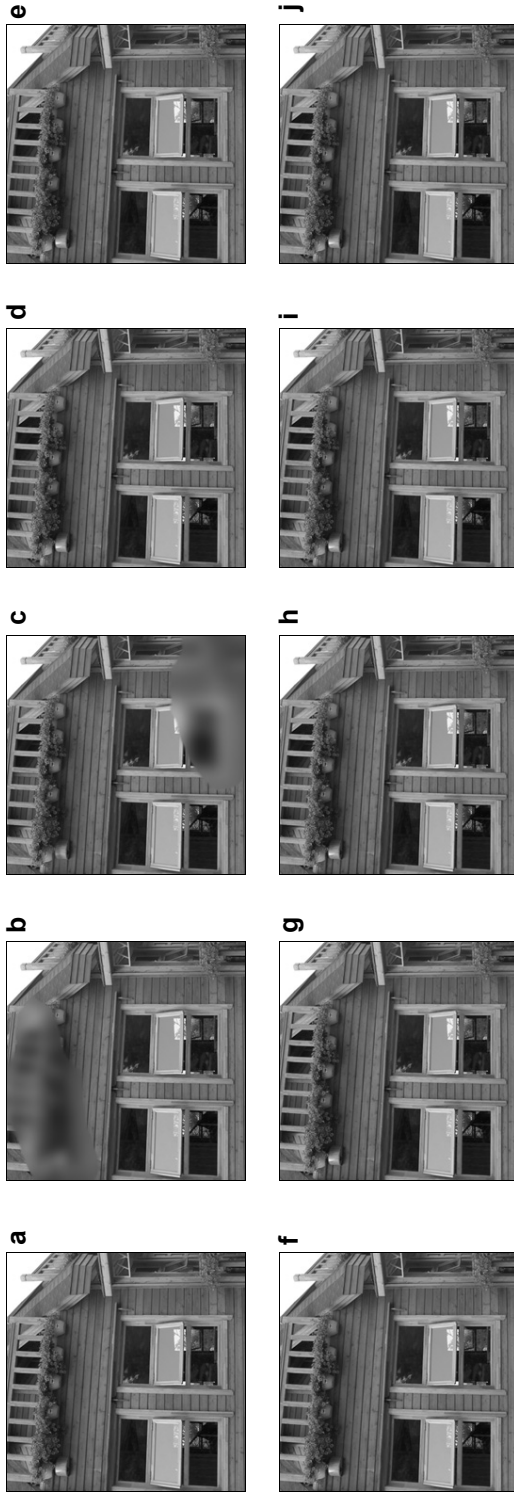
Fig. 3. Example of multi-focus image fusion. **a** – reference image (all in focus); **b** – source image (focused on the bottom); **c** – source image (focused on the top); **d** – fused image obtained by DWT; **e** – fused image obtained by CT; **f** – fused image obtained by NSCT; **g** – fused image (corresponding to minimum of RMSE) obtained by GA; **i** – fused image (corresponding to minimum of RMSE) obtained by NSCT-PCNN; **h** – fused image (corresponding to minimum of RMSE) obtained by BPSO; **j** – fused image (corresponding to minimum of RMSE) obtained by QPSO.

T a b l e 1. Objective fusion performance of DWT, CT, and NSCT-PCNN algorithm.

Algorithm	Evaluation metrics					
	RMSE	SF	EOG	MI	$Q^{AB/F}$	Time [s]
DWT	7.3968	23.3196	546.5472	4.3888	0.8945	0.1280
CT	4.1621	23.4209	551.4273	4.2131	0.9030	1.1594
NSCT	5.0628	23.2031	549.2036	4.8573	0.9148	103.3766
NSCT-PCNN	3.2326	23.3571	548.3018	5.3076	0.9261	74.0174

T a b l e 2. Objective fusion performance of BPSO and QPSO algorithm (Avg: average results of 100 repeated runs).

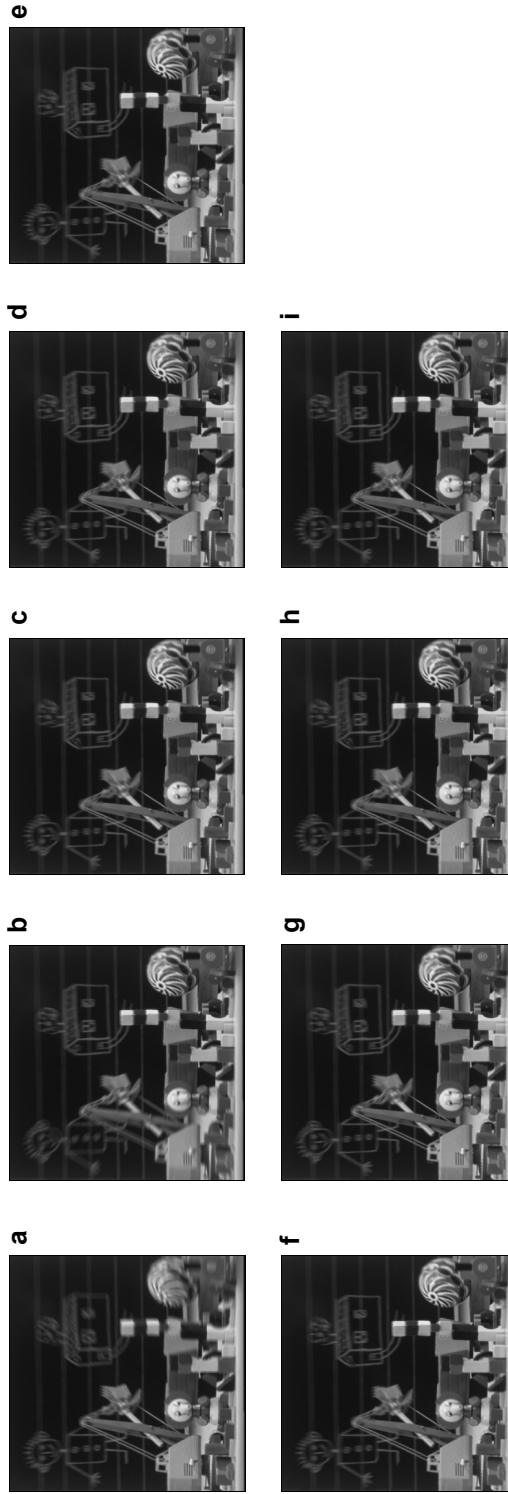| Algorithm	Min(RMSE)	Evaluation metrics					
		Avg(RMSE)	Avg(SF)	Avg(EOG)	Avg(MI)	Avg($Q^{AB/F}$)	Avg(Time [s])
GA	0	1.6933	23.4316	551.8223	7.2106	0.9365	0.2012
BPSO	0	1.9439	23.4337	552.5105	7.2119	0.9365	0.1874
QPSO	0	1.6932	23.4319	551.8379	7.2143	0.9368	0.1003

Fig. 4. Example of digital camera multi-focus image fusion. **a** – source image (focus on the left); **b** – source image (focus on the right); **c** – fused image obtained by DWT algorithm; **d** – fused image obtained by CT algorithm; **e** – fused image obtained by NSCT algorithm; **f** – fused image obtained by NSCT-PCNN algorithm; **g** – fused image obtained by GA algorithm; **h** – fused image obtained by BPSO algorithm; **i** – fused image obtained by QPSO algorithm.

In Tables 1 and 2, we can see that the fused images of DWT, CT, NSCT and NSCT-PCNN all have some small errors according to RMSE, while QPSO as well as GA and BPSO methods can accomplish absolute restoration with RMSE = 0. Furthermore, when compared to the average value of RMSE, QPSO achieves the smallest value. That is to say, the proposed method is a satisfied fusion technique with smaller error. According to EOG and SF, there is not much difference among all used methods. However, the indexes MI and $Q^{AB/F}$ indicate that GA, BPSO and QPSO performance is more advantageous than the former four methods in obtaining information from the source images. That also means, QPSO improves the convergence ability. We can see that NSCT and NSCT-PCNN methods are the most time-cost; QPSO has the fastest execution speed. In house images test, QPSO improves 50.1% speed of GA and 46.5% speed of BPSO.

4.2. Digital camera multi-focus images application

In practice, images are usually captured by digital cameras. As the limited depth-of--field, it is often not possible to get an image that contains all relevant objects sharply focused. And the multi-focus digital camera images are usually not registered. So it is an important issue to study multi-focus image fusion of digital camera images.

In this section, the experiment is performed on a set of images acquired by a real lens. The toy images (size of 512×512) are as shown in Fig. 4. It is without a reference image. Table 3 presents the fusion results of DWT, CT, NSCT, NSCT-PCNN, GA, BPSO and QPSO methods.

T a b l e 3. Objective fusion performance.

Algorithm	Evaluation metrics				
	EOG	SF	MI	$Q^{AB/F}$	Time [s]
DWT	220.9301	29.6432	6.3561	0.6813	0.4006
CT	218.1479	29.4559	7.1671	0.7203	5.5720
NSCT	219.4097	29.5405	7.1036	0.7225	433.6872
NSCT-PCNN	214.5736	29.2129	7.3271	0.7283	317.9738
GA	213.5696	29.1451	8.6779	0.7567	1.1224
BPSO	214.2117	29.1887	8.6728	0.7557	0.8592
QPSO	213.4527	29.1371	8.6874	0.7567	0.3407

As illustrated in Table 3, we can see that QPSO performs excellent fusion and has the fastest speed. In indexes MI and $Q^{AB/F}$, QPSO gets larger value as well as GA and BPSO methods, which means it can extract more legible information from source images. According to the other four evaluation measures, the fused image definition of QPSO method is either better or worse than the other methods. It is proved that QPSO method achieves satisfactory performance from both the visual and statistical standpoints. From Table 3, we can see that the run time of QPSO method is 0.3407 s, which is the shortest. Compared with other methods, it decreases by 14.95%, 93.88%,

99.92%, 99.89%, 69.64% and 60.35% of DWT, CT, NSCT, NSCT-PCNN, GA and BPSO, respectively. These data demonstrate that QPSO is an excellent optimization technique with high speed.

5. Conclusions

In this paper, a new intelligent particle swarm search strategy QPSO is presented and applied in the field of multi-focus image fusion. The proposed method is a variant of basic particle swarm optimization inspired by quantum mechanism, especially with stronger search ability and accelerated executing speed. Several artificial and digital camera multi-focus images are employed in experience to analyze the performance of QPSO. When compared with the previous methods, we use objective definition measures to evaluate the fusion performance, and time to compare the instantaneity of methods. The experience results of artificial image fusion show that QPSO method can realize absolute restoration with zero error, when compared to the reference images. Besides, the digital image fusion results demonstrate that QPSO method can optimize fusion of multi-focus image. And both kinds of experience show QPSO has superior execution speed. So we can conclude the proposed method is an adaptive and reliable image fusion technique with high speed and high accuracy.

References

[1] SHUTAO LI, BIN YANG, *Multifocus image fusion using region segmentation and spatial frequency*, Image and Vision Computing **26**(7), 2008, pp. 971–979.

[2] JING TIAN, LI CHEN, *Adaptive multi-focus image fusion using a wavelet-based statistical sharpness measure*, Signal Processing **92**(9), 2012, pp. 2137–2146.

[3] SHUTAO LI, BIN YANG, JIANWEN HU, *Performance comparison of different multi-resolution transforms for image fusion*, Information Fusion **12**(2), 2011, pp. 74–84.

[4] ZHAOBIN WANG, YIDE MA, JASON GU, *Multi-focus image fusion using PCNN*, Pattern Recognition **43**(6), 2010, pp. 2003–2016.

[5] XIAO-BO QU, JING-WEN YAN, HONG-ZHI XIAO, ZI-QIAN ZHU, *Image fusion algorithm based on spatial frequency-motivated pulse coupled neural networks in nonsubsampled contourlet transform domain*, Acta Automatica Sinica **34**(12), 2008, pp. 1508–1514.

[6] XINMAN ZHANG, LUBING SUN, JIUQIANG HAN, GANG CHEN, *An application of swarm intelligence binary particle swarm optimization (BPSO) algorithm to multi-focus image fusion*, Optica Applicata **40**(4), 2010, pp. 949–964.

[7] XINMAN ZHANG, JIUQIANG HAN, PEIFEI LIU, *Restoration and fusion optimization scheme of multifocus image using genetic search strategies*, Optica Applicata **35**(4), 2005, pp. 927–942.

[8] YUJIE CAI, JUN SUN, JIE WANG, YANRUI DING, NA TIAN, XIANGRU LIAO, WENBO XU, *Optimizing the codon usage of synthetic gene with QPSO algorithm*, Journal of Theoretical Biology **254**(1), 2008, pp. 123–127.

[9] KE MENG, HONG GANG WANG, ZHAOYANG DONG, KIT PO WONG, *Quantum-inspired particle swarm optimization for valve-point economic load dispatch*, IEEE Transactions on Power Systems **25**(1), 2010, pp. 215–222.

[10] FANG LIU, HAIBIN DUAN, YIMIN DENG, *A chaotic quantum-behaved particle swarm optimization based on lateral inhibition for image matching*, Optik – International Journal for Light and Electron Optics **123**(21), 2012, pp. 1955–1960.

[11] YI CHAI, HUAFENG LI, ZHAOFEI LI, *Multifocus image fusion scheme using focused region detection and multiresolution*, Optics Communications **284**(19), 2011, pp. 4376–4389.

[12] WEI HUANG, ZHONGLIANG JING, *Evaluation of focus measures in multi-focus image fusion*, Pattern Recognition Letters **28**(4), 2007, pp. 493–500.